

## OBSERVATION OF SMITH-PURCELL RADIATION AT 32 GHZ FROM A MULTI-CHANNEL GRATING WITH SIDEWALLS

J. T. Donohue, CENBG, CNRS/IN2P3, Université de Bordeaux, France  
J. Gardelle, P. Modin, CEA, CESTA, Le Barp, France

### Abstract

In a demonstration experiment at 5 GHz, we found copious emission of coherent Smith-Purcell (SP) radiation at the fundamental frequency of the evanescent surface wave, when the grating had sidewalls. Reaching higher frequencies requires a reduction in the size of the grating, which leads to a considerable reduction in power. To partially compensate this, we suggested superposing several copies of the reduced grating in parallel. A test of this concept has been performed with a seven-channel grating, at a frequency near 32 GHz. The SP radiation signals were observed directly with a fast oscilloscope. Power levels were of order 5 kW, in fair agreement with three-dimensional simulations made with the code "MAGIC".

### INCREASE FREQUENCY BY REDUCING THE PERIOD AND WIDTH BETWEEN SIDEWALLS

A demonstration experiment in the microwave domain showed that a Smith-Purcell (SP) free electron laser (FEL), with conducting sidewalls placed at the ends of the grating's grooves, emitted intense radiation at the frequency of the surface wave on the grating [1]. In single shot operation, the ratio of emitted power to beam power exceeded 10 %. An earlier experiment, on a grating without sidewalls [2], had demonstrated emission of coherent SP radiation at the second harmonic of the surface wave. That experiment confirmed the scenario proposed in the two-dimensional (2-D) model of Andrews and Brau [3]. But the efficiency was only of order 0.1 %. In the presence of sidewalls the dispersion relation for the grating surface wave is modified [4]. In particular, the intersection of the beam line with the new dispersion relation may occur at an allowed SP frequency, which can't happen in the 2-D theory of Reference [3]. Since the beam bunching at the fundamental frequency is typically much greater than that on harmonics, the emission at the fundamental frequency is much stronger. Thus the use of sidewalls greatly increases the power. Of course, to be of practical interest, it is necessary to reach much higher frequencies, i.e., mm wavelength or less.

The well-known SP relation is [5],

$$\lambda = L(1/\beta - \cos \theta_{SP})/|n|,$$

where  $\lambda$  denotes the wavelength,  $L$  the grating period,  $n$  the order of diffraction,  $\theta_{SP}$  the angle with respect to the beam, and  $\beta$  the relative velocity of the electron. In order to reach shorter wavelengths, it suffices to reduce the grating period. However, the component of the evanescent surface wave in resonance with the beam only

extends to a height proportional to the wavelength. In order to reach high frequencies, the beam must closely approach the grating surface. If the grating profile is preserved (groove-depth/period and groove-width/period constant), the 2D dispersion relation of Andrews and Brau in the dimensionless variables is unchanged. The scale reduction doesn't require a reduction in the overall size of the grating, although the task of propagating an intense and wide sheet beam at tiny distances above the grating would certainly be difficult. For the grating with sidewalls, the distance between sidewalls,  $w$ , must undergo the same reduction in scale as the period  $L$ . This rapidly leads to long thin gratings when the frequency is increased. Furthermore, our experiment requires an intense (0.5 T) longitudinal magnetic field to control the beam. At the portion of the beam nearest the grating, the image charges produce a moderately strong vertical electric field (a few kV/cm), which, combined with the magnetic field, generates a transverse  $\vec{E} \times \vec{B}$  drift. If the number of periods is too great, most of the electrons will drift into the sidewalls. If the radiated intensity is proportional to the total surface of the grating, a grating with sidewalls will suffer a power reduction proportional to the square of the scale factor.

At FEL 2013 two of the authors suggested that it might be possible to superpose laterally  $N$  copies of the  $N$ -fold reduced gratings [6]. The beam used in the full-scale experiment would continue in use, except that it would be positioned to be flush with the grating top, and of 1 mm thickness. The hope was that the overall power reduction would be only  $1/N$ , instead of  $1/N^2$ . In support of this hypothesis, several simulations of multi-channel gratings were performed with the three-dimensional (3D) particle-in-cell code "MAGIC" [7]. These simulations, made with 2, 4, 6, 8 and 10 channels, indicated that the radiation at the bunching frequency ( $N$  times the original bunching frequency) occurred at the same SP angle, which was approximately  $140^\circ$ . On the upstream wall of the simulation volume, the azimuthal distribution grew more concentrated around the vertical direction with increasing  $N$ . A simple analysis using the theory of antenna arrays was proposed to explain this tendency. It indicated that the width of the azimuthal distribution would decrease as  $1/N$ , as would the radiated power in the principal lobe

These results depend crucially on the existence of some coherence among the various channels. In the antenna theory this is assumed, but in the simulations, it is seen to be only a fair approximation. Although the simulated fields from each channel merge smoothly into the observed radiation pattern, there is no reason to expect this to occur in practice. It then becomes necessary to

confirm that enough coherence takes place to produce a well-collimated radiation pattern. To test this, we carried out an experiment on a seven-channel grating with sidewalls at a frequency of approximately 32 GHz.

### DESCRIPTION OF THE EXPERIMENT

Our previous work at frequencies of order 5 GHz used standard microwave detectors and oscilloscopes that were available. To reach higher frequency, the possibility of using a 33 GHz bandwidth oscilloscope (DSA73304) suggested dimensioning the experiment to produce radiation near 32 GHz. The dimensions of our previous and new gratings are shown in the Table.

Table 1: Parameters of the Experiment

Parameters	Original grating	7-channel grating
Peak Voltage	60-120 kV	60-120 kV
Current	10-40 A	10-40 A
Pulse duration FWHM	300 ns	300 ns
Beam thickness	1 mm	1-2 mm
Beam height	0.5 mm	0-2 mm
Beam width	3.5 cm	5.2 cm
Period $L$	2 cm	3.3 mm
Groove depth $H$	1 cm	1.65 mm
Groove width $A$	1 cm	1.65 mm
Channel width $w$	4 cm	6.6 mm
Number of periods	20	40
Magnetic field	1 T	0.5 T

The dispersion relation (DR) for the grating is displayed in Fig. 1, along with the 2-D DR of Andrews and Brau. For beam energy of 80 keV, the operating point is at 33.2 GHz. The corresponding SP angle is 145°.

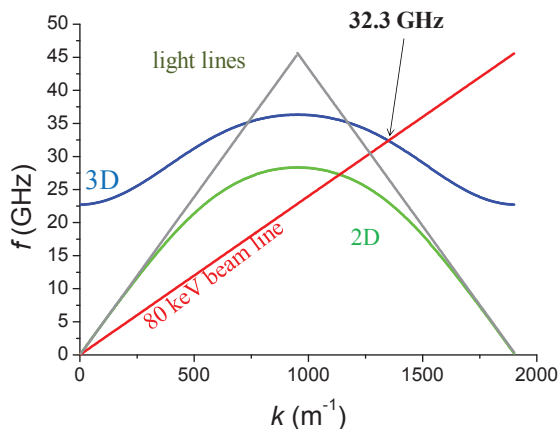


Figure 1: Dispersion relation: frequency  $f$  v. axial wave number  $k$ , for grating with  $L = w/2 = 3.3$  mm. 2D green, 3D blue, 80 keV beam line red.

The set-up may be seen in Fig. 2. The radiation enters a section of WR 28 wave guide surrounded by a flange. A small B-dot probe is positioned near the grating so as to measure the magnetic field a few mm above the grating. The return current from the beam stop is monitored by a Rogowski coil.

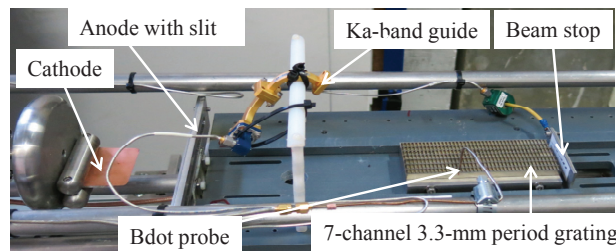


Figure 2: Photograph of set-up, showing essential elements. The vacuum box and solenoid are not shown.

The sheet beam is emitted from a knife-edge cathode, and passes through a slit on the anode, whose height and opening width may be adjusted. Thermally sensitive paper on the beam stop can be used to observe the beam shape. The experiment is inserted in a cylindrical vacuum box, which is surrounded by a pulsed solenoid.

A major concern is the efficiency of the wave guide and flange system for detecting the SP radiation. To investigate this 3D “MAGIC” were performed. One is displayed in Fig. 3.

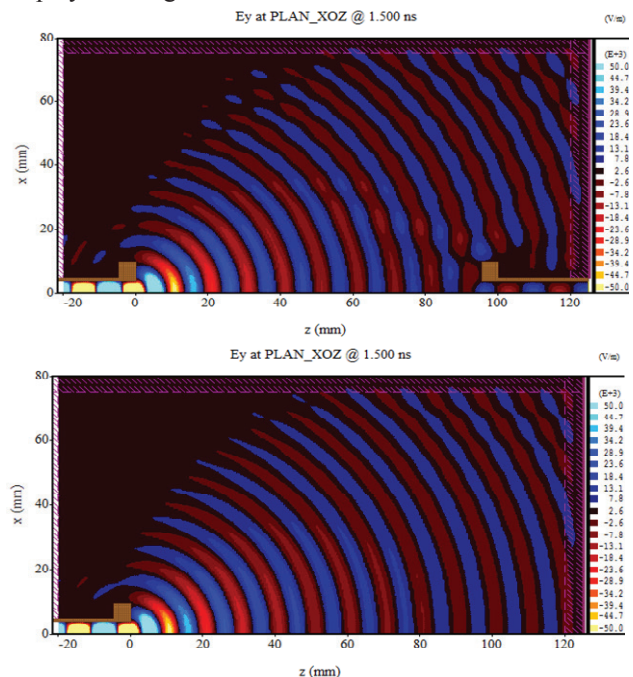


Figure 3: Waveguide efficiency “MAGIC” simulations: upper with and lower without wave guide receiver.

An input wave guide emits radiation at 33 GHz on the bottom left. The upper figure shows the propagation from the wave guide source to a similar detector at the bottom right. The lower shows the power flow in the absence of the receiver. We find that the power in the wave guide overestimates by a factor of 1.5 (at 33 GHz) the power arriving in the equivalent area in the second simulation. This correction factor was included in our power estimates.

The attenuation of the connecting cables and fixed attenuators was measured as a function of frequency by using a tunable source of known power connected to the oscilloscope. The response of the B-dot probe (located

just above a groove of the grating) was estimated from its calculated inductance and area, with an error of 20%.

In Fig. 4 contour map of  $B_x$  is displayed in order to show where the radiation is predicted to occur (145°). The Ka-band waveguide has been moved around this lobe.

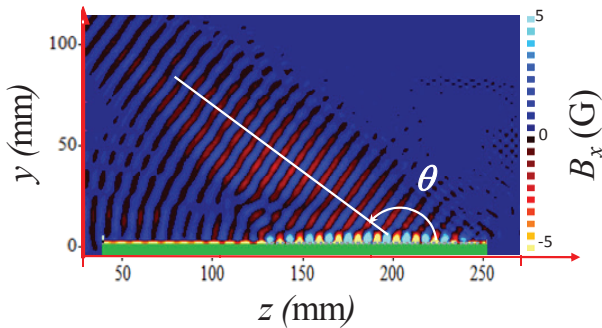


Figure 4: "MAGIC" contour map of  $B_x$  showing angle of emission.

### RESULTS OF THE EXPERIMENT

In Fig. 5, we have plotted the two oscilloscope signals, B-dot (left scale) and Ka-band (right scale), for two shots. We observe a shot-to-shot variation due to fluctuations in beam current. There is considerable resemblance between the signals.

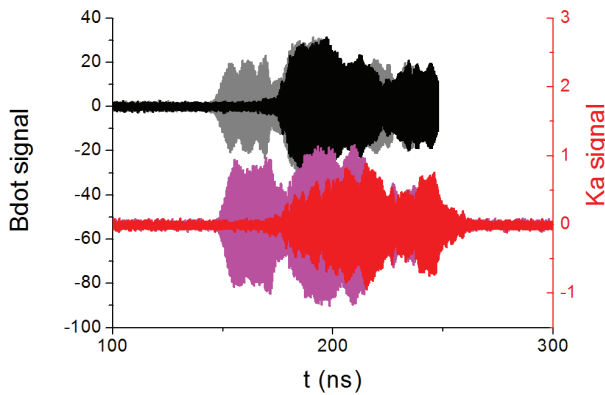


Figure 5: Comparison of the B-dot (left scale) and Ka-band signals (right scale) for two different shots.

By using our calibration of the B-dot probe, we show in Fig. 6 a typical magnetic component  $B_x$  as a function of time, along with its FFT. The maximum value is in good agreement with MAGIC predictions at the B-dot location. The measured frequency corresponds to that expected from the dispersion relation.

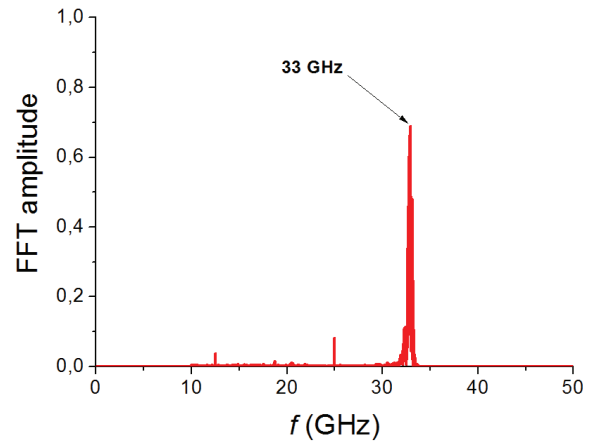
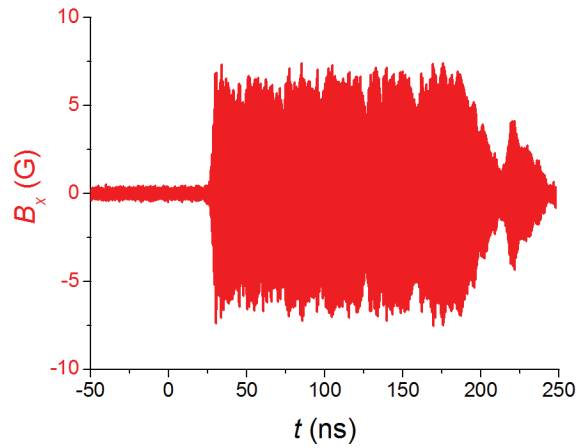
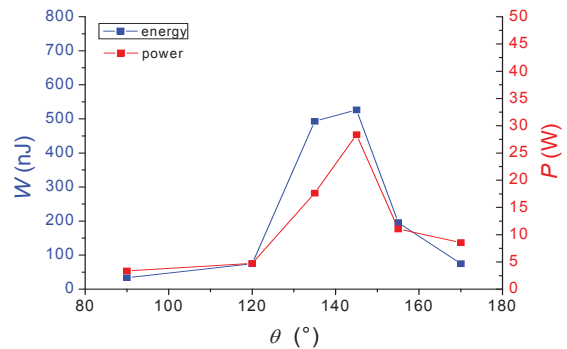


Figure 6:  $B_x$  field from the B-dot time signal and FFT.

The Ka-band wave guide was moved so as to explore the radiation pattern. We present in Fig. 7 some results of this exploration: the top figure gives the variation in  $\theta$  at  $\phi = 90^\circ$  whereas the lower figure gives the variation in  $\phi$  at  $\theta = 145^\circ$ . Both the peak instantaneous power (red) and the energy (blue) are plotted. The energy is deduced by integrating the power over the duration of the pulse.



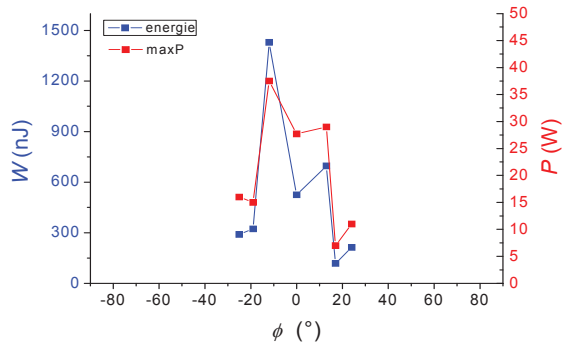


Figure 7: Angular distributions of energy and power.

We can compare this value to the MAGIC simulation which is displayed in Fig. 8. This 3D plot shows the power density in a plane at the position  $z = 6$  cm (as shown in Fig. 4). In this simulation, which uses a perfect grazing beam at 20 A, the power density is of the same order of magnitude and leads to a total emitted power of approximately 20 kW.

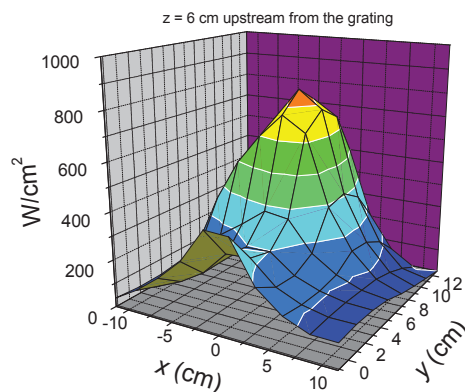


Figure 8: “MAGIC” prediction for power distribution on the rear wall of the simulation volume.

The radiation pattern depends strongly on the coherence among the different channels. If the coherence is high the radiation is confined to a relatively narrow lobe. However, we have no general argument that such coherence is to be expected, and we rely on simulations that suggest that a fair degree of coherence occurs. We varied the mesh size to see whether the coherence depended upon it. Unfortunately, it does. The results of this investigation are displayed in Fig. 9.

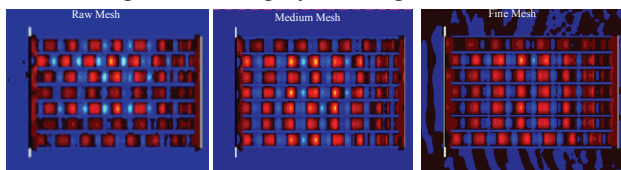


Figure 9: Influence of mesh-size on coherence.

Here we show the contour maps of  $B_x$  at the top of grating surface for three different mesh size in the

direction along the grooves (1330, 570 and 290  $\mu\text{m}$ , from left to right). The smallest mesh size is the practical limit of the computer we used. We can see that the coherence is better for the smallest mesh size though not perfect. However, the effect of coherence is to concentrate the emission pattern into a narrow lobe by limiting the azimuthal angle  $\phi$  to small values around  $90^\circ$ . The experimental results indicate that the power is indeed concentrated in such a small lobe

## CONCLUSION

The results presented here lend support to the hypothesis that a multi-channel SP FEL with sidewalls has enough coherence to produce a reasonably narrow radiation pattern. The concentration around the SP angle with respect to the beam direction was to be expected, while the concentration in a narrow range of azimuthal angle happens only if substantial coherence among the different channels occurs. Although we know of no general argument in favour of such coherence, it appears to occur both in our somewhat rough experiment as well in the simulations with small transverse mesh-size. In the near future a 20 channel grating designed to produce radiation at 100 GHz will be tested.

## REFERENCES

- [1] J. Gardelle, P. Modin and J. T. Donohue, "Observation of copious emission at the fundamental frequency by a Smith-Purcell free-electron laser with sidewalls", *Appl. Phys. Lett.* **100**, 111303 (2012).
- [2] J. Gardelle, L. Courtois, P. Modin and J. T. Donohue, "Observation of coherent Smith-Purcell radiation using an initially continuous flat beam", *Phys. Rev. ST Accel. Beams* **12**, 110701 (2009).
- [3] H. L. Andrews and C. A. Brau, "Gain of a Smith-Purcell free-electron laser", *Phys. Rev. ST Accel. Beams* **7**, 070701 (2004).
- [4] J. T. Donohue and J. Gardelle, *Phys. Rev. ST Accel. Beams* **14**, 060709 (2011).
- [5] S. J. Smith and E. M. Purcell, "Visible light from localized surface charges moving across a grating", *Phys. Rev.* **92**, 1069 (1953).
- [6] J. T. Donohue and J. Gardelle, "Towards high frequency operation with a multi-grating Smith-Purcell Fel" in *Proc. 35th Int. Free-Electron Laser Conf.*, New York, 2013, pp. 525-528.
- [7] B. Goplen, L. Ludeking, D. Smithe, and G. Warren, "User-configurable MAGIC for electromagnetic PIC calculations", *Computer Physics Communications* **87**, 54 (1995).